

Decentralized real time implementation of a Leader-Follower coordination strategy for quadrotors

José J. Corona-Sánchez, Juan A. Vargas-Jacob and H. Rodríguez-Cortés

Abstract—This paper presents a decentralized real time implementation of a leader-follower multiagent coordination strategy for quadrotors. The distance from the leader to the followers is specified by a set of interagent distances. Each agent maintains its desired position by means of a distributed trajectory generator in conjunction with local robust nonlinear controllers. The decentralized real time implementation is based on the Giotto model for embedded systems. The performance of the leader-follower coordination strategy is verified experimentally using two quadrotors.

I. INTRODUCTION

For missions such as monitoring, surveillance, search, rescue, and cooperative transportation; fault tolerance and efficiency are attractive characteristics of employing multiagent systems, instead of a single complicated system. However, the success of such missions depends on the adequate coordination of the multiagent system. Multiagent coordination has been addressed mainly from three different frameworks: leader-following, behavioral, and virtual structures [7]. The resulting coordination strategies have been implemented using centralized or decentralized configurations depending on the hardware availability and the circumstances of the mission. It is commonly accepted that the decentralized implementation has more potentiality for real applications, although the complexity increases considerably.

In the last years the problem of coordinating multiagent systems has been a very active field of research, thus many interesting results have been obtained [17], [9], [18], [25]. In the literature, experimental work of multiagent coordination strategies has been performed with mobile robots, fixed wing aircrafts, helicopters, satellites, and lately with quadrotors.

Quadrotors are promising aerial vehicles for diverse applications due to their mechanical simplicity and capability for indoor as well as outdoor operation. Many solutions for the control problems of regulation, trajectory tracking and path following for the quadrotor have been proposed in the literature. For instance, feedback linearization control [1], [5], Lyapunov based output feedback [16], backstepping [12], [8], [11], nested saturations [4], [21], sliding mode control [24] and a non-linear \mathcal{H}_∞ control [19] and path following [15].

Some solutions for coordination of multiagent systems composed of quadrotors have been also proposed. For in-

stance in [23] a centralized configuration of a multiagent aggressive formation flight strategy is presented. The effects of time delays in the network and communication failures on the multiagent performance are evaluated. Experimental work supports the performance of the proposed coordination strategy. In [6] a leader following coordination strategy is presented. The implementation combines a sliding mode controller for the translational dynamics in conjunction with a proportional derivative controller for the rotational dynamics. Experimental results using a virtual leader are presented. Using the notions of graph rigidity and persistence as well as techniques of virtual target tracking and smooth switching a multiagent formation strategy is proposed in [3]. The proposed formations strategies are applied to multiagent systems composed of quadrotors as well as fixed wing aircraft. Numerical simulations are proposed to illustrate the performance of their multiagent formations strategies.

This paper presents a decentralized real time implementation of a leader-follower coordination scheme with two aerial vehicles powered by four rotors. The distance from the leader to the followers is specified by a set of interagent distances. Each agent maintains its desired position by means of a distributed trajectory generator in conjunction with local robust nonlinear controllers. The decentralized real time implementation is based on the Giotto model for embedded systems. The performance of the leader-follower coordination strategy is verified experimentally using two quadrotors. It is important to underscore that we consider for coordination only the spatial position of the quadrotor, we assume that the yaw angle is commanded by the local controllers to be at zero.

The rest of this paper is organized as follows. In Section 2 a brief glance of the quadrotor mathematical model is presented. Section 3 presents the developments related to the coordination strategy. Section 4 is devoted to the real time decentralized implementation of the leader-follower coordination scheme. In Section 5 a series of experimental results are presented. Finally, in Section 6 some concluding remarks are presented.

II. THE QUADROTOR

A. Model of the quadrotor agents

The quadrotor vehicle is powered by four rotors attached to a cross shaped mechanical structure. This configuration provides full actuation to the rotational dynamics, however the translational dynamics remains under actuated. The quadrotor dynamic model can be described like a rigid body moving in the space. Defining $0x^e y^e z^e$ the right-hand inertial

H. Rodríguez-Cortés and Juan A. Vargas-Jacob are with the Centro de Investigación y de Estudios Avanzados del Instituto Politécnico Nacional, Av. IPN 2508, San Pedro Zacatenco, 07360, México, D.F., México. José J. Corona-Sánchez is with the ESIME Azcapotzalco, Av. Granjas 682, Santa Catarina, Azcapotzalco, 02250, México, D.F. México {jjcorona, jvargas, hrodriguez}@cinvestav.mx

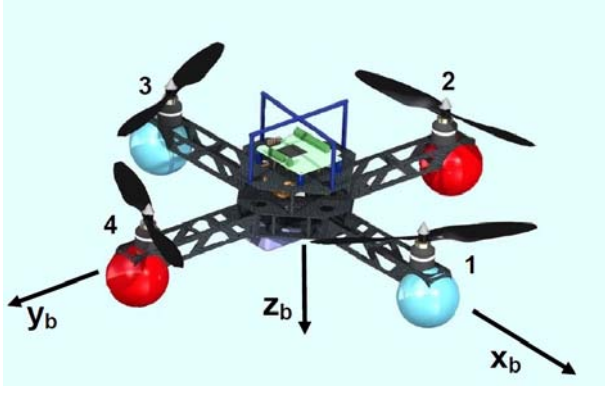


Fig. 1. Quadrotor helicopter

frame with z^e pointing downwards into the earth and x_e pointing to the East, and $0x^b y^b z^b$ the right-hand frame fixed to the center of mass of the aircraft structure (body frame) with x^b and y^b pointing in the direction of the structure's arms, see Figure 1.

The agent dynamics expressed in mixed inertial and body coordinates is described by

$$\begin{aligned} m_i \ddot{X}_i &= \begin{bmatrix} -T_{T_i} (c_{\psi_i} s_{\theta_i} c_{\phi_i} + s_{\psi_i} s_{\phi_i}) \\ -T_{T_i} (s_{\psi_i} s_{\theta_i} c_{\phi_i} - c_{\psi_i} s_{\phi_i}) \\ m_i g - T_{T_i} c_{\theta_i} c_{\phi_i} \end{bmatrix} + \delta_{T_i} \\ \dot{\Phi}_i &= W_i^{-1} \Omega_i \\ J_i \dot{\Omega}_i &= -\Omega_i \times J_i \Omega_i + \begin{bmatrix} (T_{3_i} - T_{1_i}) \ell \\ (T_{2_i} - T_{4_i}) \ell \\ Q_{T_i} \end{bmatrix} + \delta_{\Omega_i} \end{aligned} \quad (1)$$

where

$$\begin{aligned} T_{T_i} &= T_{1_i} + T_{2_i} + T_{3_i} + T_{4_i} \\ Q_{T_i} &= Q_{1_i} - Q_{2_i} + Q_{3_i} - Q_{4_i} \\ W_i^{-1} &= \begin{bmatrix} 1 & t_{\theta_i} s_{\phi_i} & t_{\theta_i} c_{\phi_i} \\ 0 & c_{\phi_i} & -s_{\phi_i} \\ 0 & \frac{s_{\phi_i}}{c_{\theta_i}} & \frac{c_{\phi_i}}{c_{\theta_i}} \end{bmatrix} \end{aligned} \quad (2)$$

Moreover, m_i is the agent mass, J_i is the agent inertia matrix, $X_i = [x_i \ y_i \ z_i]^\top$ is the position of the agent's center of gravity, $\Phi_i = [\phi_i \ \theta_i \ \psi_i]^\top$ is the agent's attitude, parameterized by Euler angles (roll, pitch, yaw), $\Omega_i = [p_i \ q_i \ r_i]^\top$ is the angular velocity of the body frame, T_{j_i} and Q_{j_i} , $j = 1, 2, 3, 4$ are the thrust and the reactive moment of the rotor j , ℓ is the distance between the agent's center of gravity and the axis of rotation of the rotor j , $\delta_{T_i} = [\delta_i^x \ \delta_i^y \ \delta_i^z]^\top$ and $\delta_{\Omega_i} = [\delta_i^p \ \delta_i^q \ \delta_i^r]^\top$ are bounded constant disturbances. Finally, $i = l, s_1, s_2, \dots, s_w$ for one leader and w followers.

III. QUADROTORS FORMATION

The main objective of formation control for multiagent systems is the design of an algorithm capable of driving each agent to a desired position with respect to the other

agents and capable of maintaining such a position when the multiagent system performs a defined task. It will be possible to design such algorithm if the agents are able to exchange information concerning their position and velocity. The information exchange between agents can be modeled with weighted directed graph [20]. Since in this paper we are considering a very simple structure for information exchange, we are not using weighted directed graphs.

We consider a multiagent system of $w + 1$ quadrotors. The coordination objective will be stated under the following assumptions

- A1 Each quadrotor in the multiagent system knows the position and velocity of its center of gravity, this is, X_i, \dot{X}_i , $i = l, s_1, \dots, s_w$ are measurable.
- A2 The follower s_i broadcast its position only to the follower s_{i+1} for $i = 1, \dots, w-1$. The leader broadcast its position only to the follower s_1 .
- A3 Only the leader knows the desired trajectory as well as the desired velocity and acceleration.
- A4 The distance between follower s_i and follower s_{i+1} is specified by the constant vector $\alpha_{s_i, s_{i+1}}$, $i = 1, \dots, w-1$. The distance between the leader and the first follower is specified by the vector α_{l, s_1} . See Figure 2.

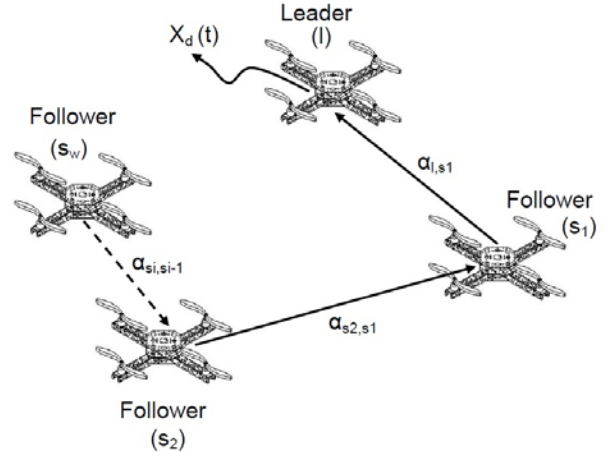


Fig. 2. Leader-Follower scheme

Now, we establish the control objective as follows.

Control objective Under assumptions A1-A4 design a control strategy such that the following holds

$$\begin{aligned} \lim_{t \rightarrow \infty} (X_{s_1} - X_l - \alpha_{l, s_1}) &= 0 \\ \lim_{t \rightarrow \infty} (X_{s_{i+1}} - X_{s_i} - \alpha_{s_i, s_{i+1}}) &= 0 \end{aligned} \quad (3)$$

for $i = 1, \dots, w-1$.

In order to address the stated control objective the formation errors are defined as follows: the leader tracking errors are

$$\begin{aligned} e_l^1 &= X_l - X_d \\ e_l^2 &= \dot{X}_l - \dot{X}_d \end{aligned}$$

while the followers formation errors are defined as

$$\begin{aligned} e_{s_1}^1 &= X_{s_1} - X_l - \alpha_{l, s_1} \\ e_{s_1}^2 &= \dot{X}_{s_1} - \dot{X}_l \end{aligned}$$

for the first follower, and

$$\begin{aligned} e_{s_i}^1 &= X_{s_i} - X_{s_{i-1}} - \alpha_{s_i, s_{i-1}} \\ e_{s_i}^2 &= \dot{X}_{s_i} - \dot{X}_{s_{i-1}}, \quad i = 2, \dots, w-1 \end{aligned}$$

for the rest of the followers. The control objective is equivalent to the objective of driving the formation errors to zero. To drive those errors to zero we use local robust nonlinear controllers for each quadrotor.

A. Local robust nonlinear controllers

The local controller for each agent is the robust nonlinear controller proposed in [14]. For the formation leader, its local nonlinear robust controller is implemented exactly as in [14]. For the followers the error dynamics take the following form

$$\begin{aligned} \dot{e}_{s_i}^1 &= e_{s_i}^2 \\ \dot{e}_{s_i}^2 &= \frac{1}{m_{s_i}} \begin{bmatrix} -T_{T_{s_i}} (c\psi_{s_i} s\theta_{s_i} c\phi_{s_i} + s\psi_{s_i} s\phi_{s_i}) \\ -T_{T_{s_i}} (s\psi_{s_i} s\theta_{s_i} c\phi_{s_i} - c\psi_{s_i} s\phi_{s_i}) \\ m_{s_i} g - T_{T_{s_i}} c\theta_{s_i} c\phi_{s_i} \end{bmatrix} \\ &\quad - \frac{1}{m_{s_{i-1}}} \begin{bmatrix} -T_{T_{s_{i-1}}} (c\psi_{s_{i-1}} s\theta_{s_{i-1}} c\phi_{s_{i-1}} + s\psi_{s_{i-1}} s\phi_{s_{i-1}}) \\ -T_{T_{s_{i-1}}} (s\psi_{s_{i-1}} s\theta_{s_{i-1}} c\phi_{s_{i-1}} - c\psi_{s_{i-1}} s\phi_{s_{i-1}}) \\ m_{s_{i-1}} g - T_{T_{s_{i-1}}} c\theta_{s_{i-1}} c\phi_{s_{i-1}} \end{bmatrix} \\ &\quad + \begin{bmatrix} \delta_{s_i}^x \\ \delta_{s_i}^y \\ \delta_{s_i}^z \end{bmatrix} - \begin{bmatrix} \delta_{s_{i-1}}^x \\ \delta_{s_{i-1}}^y \\ \delta_{s_{i-1}}^z \end{bmatrix} \end{aligned} \quad (4)$$

for $i = 1, \dots, m$ with $s_0 = l$. Following the developments in [14] we define

$$\begin{aligned} \frac{1}{m_{s_i}} \begin{bmatrix} -T_{T_{s_i}} (c\psi_{s_i} s\theta_{s_i} c\phi_{s_i} + s\psi_{s_i} s\phi_{s_i}) \\ -T_{T_{s_i}} (s\psi_{s_i} s\theta_{s_i} c\phi_{s_i} - c\psi_{s_i} s\phi_{s_i}) \\ m_{s_i} g - T_{T_{s_i}} c\theta_{s_i} c\phi_{s_i} \end{bmatrix} &= \begin{bmatrix} \gamma_{s_i}^x \\ \gamma_{s_i}^y \\ \gamma_{s_i}^z \end{bmatrix} \\ -(g - \gamma_{s_i}^z) \begin{bmatrix} c\psi_{s_i} & s\psi_{s_i} & 0 \\ c\psi_{s_i} & -c\psi_{s_i} & 0 \\ 0 & 0 & 0 \end{bmatrix} \begin{bmatrix} t\theta_{s_i} - t\theta_{s_i}^d \\ t\phi_{s_i} - t\phi_{s_i}^d \\ c\phi_{s_i} \end{bmatrix} & \end{aligned} \quad (5)$$

This is achieved with

$$\begin{aligned} T_{T_{s_i}} &= \frac{m_{s_i} (g - \gamma_{s_i}^z)}{c\theta_{s_i} c\phi_{s_i}} \\ \phi_{s_i}^d &= \frac{c\theta_{s_i} (s\psi_{s_i} \gamma_{s_i}^x - c\psi_{s_i} \gamma_{s_i}^y)}{g - \gamma_{s_i}^z} \\ \theta_{s_i}^d &= \frac{c\psi_{s_i} \gamma_{s_i}^x + s\psi_{s_i} \gamma_{s_i}^y}{g - \gamma_{s_i}^z} \end{aligned}$$

where $\gamma_{s_i}^j$, $j = x, y, z$ are the new control inputs. Hence, the closed-loop dynamics (4)-(5) takes the following form

$$\begin{aligned} \dot{e}_{s_i}^1 &= e_{s_i}^2 \\ \dot{e}_{s_i}^2 &= \begin{bmatrix} \gamma_{s_i}^x \\ \gamma_{s_i}^y \\ \gamma_{s_i}^z \end{bmatrix} - \begin{bmatrix} \gamma_{s_{i-1}}^x \\ \gamma_{s_{i-1}}^y \\ \gamma_{s_{i-1}}^z \end{bmatrix} \\ &\quad - (g - \gamma_{s_i}^z) \begin{bmatrix} c\psi_{s_i} & s\psi_{s_i} & 0 \\ c\psi_{s_i} & -c\psi_{s_i} & 0 \\ 0 & 0 & 0 \end{bmatrix} \begin{bmatrix} t\theta_{s_i} - t\theta_{s_i}^d \\ t\phi_{s_i} - t\phi_{s_i}^d \\ c\phi_{s_i} \end{bmatrix} \\ &\quad + (g - \gamma_{s_{i-1}}^z) \begin{bmatrix} c\psi_{s_{i-1}} & s\psi_{s_{i-1}} & 0 \\ c\psi_{s_{i-1}} & -c\psi_{s_{i-1}} & 0 \\ 0 & 0 & 0 \end{bmatrix} \begin{bmatrix} t\theta_{s_{i-1}} - t\theta_{s_{i-1}}^d \\ t\phi_{s_{i-1}} - t\phi_{s_{i-1}}^d \\ c\phi_{s_{i-1}} \end{bmatrix} \\ &\quad + \begin{bmatrix} \delta_{s_i}^x \\ \delta_{s_i}^y \\ \delta_{s_i}^z \end{bmatrix} - \begin{bmatrix} \delta_{s_{i-1}}^x \\ \delta_{s_{i-1}}^y \\ \delta_{s_{i-1}}^z \end{bmatrix} \end{aligned} \quad (6)$$

Each local controller has a disturbance estimator, to design such an estimator we define the disturbance estimator error as follows

$$\eta_{s_i} = \delta_{T_{s_i}} - \bar{\delta}_{T_{s_i}} \tanh \left(\frac{\hat{\delta}_{T_{s_i}} - \beta_{s_i}(\dot{X}_{s_i})}{\bar{\delta}_{T_{s_i}}} \right) \quad (7)$$

where $\bar{\delta}_{T_{s_i}}$ is an upper bound of the disturbance which is assumed to be known, $\hat{\delta}_{T_{s_i}}$ is the state of the disturbance estimator which will be defined in the following as well as the function $\beta_{s_i}(\dot{X}_{s_i})$. Thus, the time derivative of η_{s_i} takes the form

$$\dot{\eta}_{s_i} = \Theta_{s_i} \left(\dot{\delta}_{T_{s_i}} - \frac{\partial \beta_{s_i}}{\partial \dot{X}_{s_i}} \ddot{X}_{s_i} \right) \quad (8)$$

where

$$\Theta_{s_i} = \frac{1}{\bar{\delta}_{T_{s_i}}} \begin{bmatrix} \alpha_{s_i}^x & 0 & 0 \\ 0 & \alpha_{s_i}^y & 0 \\ 0 & 0 & \alpha_{s_i}^z \end{bmatrix}$$

with $\alpha_{s_i}^k = \bar{\delta}_{T_{s_i}}^2 - (\dot{k}_{s_i} - \delta_{s_i}^k)^2$, $k = x, y, z$. The estimation strategy is based on the Immersion and Invariance technique [2] and its objective is to asymptotically drive η_{s_i} to zero, since in this case it follows that

$$\lim_{t \rightarrow \infty} \left[\bar{\delta}_{T_{s_i}} \tanh \left(\frac{\hat{\delta}_{T_{s_i}} - \beta_{s_i}(\dot{X}_{s_i})}{\bar{\delta}_{T_{s_i}}} \right) \right] = \delta_{T_{s_i}} \quad (9)$$

In order to achieve the estimation objective $\hat{\delta}_{T_{s_i}}$ and $\beta_{s_i}(e_{s_i}^2)$ are defined as follows

$$\begin{aligned} \hat{\delta}_{T_{s_i}} &= \frac{1}{m_{s_i}} \frac{\partial \beta_{s_i}}{\partial \dot{X}_{s_i}} \begin{bmatrix} -T_{T_{s_i}} (c\psi_{s_i} s\theta_{s_i} c\phi_{s_i} + s\psi_{s_i} s\phi_{s_i}) \\ -T_{T_{s_i}} (s\psi_{s_i} s\theta_{s_i} c\phi_{s_i} - c\psi_{s_i} s\phi_{s_i}) \\ m_{s_i} g - T_{T_{s_i}} c\theta_{s_i} c\phi_{s_i} \end{bmatrix} \\ &\quad + \bar{\delta}_{T_{s_i}} \tanh \left(\frac{\hat{\delta}_{T_{s_i}} - \beta_{s_i}(\dot{X}_{s_i})}{\bar{\delta}_{T_{s_i}}} \right) \end{aligned} \quad (10)$$

and

$$\beta_{s_i}(\dot{X}_{s_i}) = \Gamma_{s_i} \dot{X}_{s_i} \quad (11)$$

with Γ_{s_i} a positive definite matrix. These definitions give the following dynamics to the disturbance estimation error

$$\dot{\eta}_{s_i} = -\Theta_{s_i} \Gamma_{s_i} \eta_{s_i} \quad (12)$$

Since Θ_{s_i} is positive definite when

$$|\delta_{T_{s_i}}| < \bar{\delta}_{T_{s_i}}$$

holds strictly, we can conclude that the estimation error converges to zero.

Now, the local controllers can be defined as follows

$$\begin{bmatrix} \gamma_{s_i}^x \\ \gamma_{s_i}^y \\ \gamma_{s_i}^z \end{bmatrix} = \begin{bmatrix} \frac{\epsilon_{s_i}^x}{2} \tanh\left(\frac{2\lambda_{s_i}^{x1}}{\epsilon_{s_i}^{x1}} e^{1x}\right) + \frac{\epsilon_{s_i}^x}{4} \tanh\left(\frac{4\lambda_{s_i}^{x2}}{\epsilon_{s_i}^{x2}} e^{2x}\right) \\ \frac{\epsilon_{s_i}^y}{2} \tanh\left(\frac{2\lambda_{s_i}^{y1}}{\epsilon_{s_i}^{y1}} e^{1y}\right) + \frac{\epsilon_{s_i}^y}{4} \tanh\left(\frac{4\lambda_{s_i}^{y2}}{\epsilon_{s_i}^{y2}} e^{2y}\right) \\ \frac{\epsilon_{s_i}^z}{2} \tanh\left(\frac{2\lambda_{s_i}^{z1}}{\epsilon_{s_i}^{z1}} e^{1z}\right) + \frac{\epsilon_{s_i}^z}{4} \tanh\left(\frac{4\lambda_{s_i}^{z2}}{\epsilon_{s_i}^{z2}} e^{2z}\right) \end{bmatrix} - \bar{\delta}_{T_{s_i}} \begin{bmatrix} \tanh\left(\frac{\hat{\delta}_{T_{s_i}}^x - \beta_{s_i}(x_{s_i})}{\delta_{T_{s_i}}}\right) \\ \tanh\left(\frac{\hat{\delta}_{T_{s_i}}^y - \beta_{s_i}(y_{s_i})}{\delta_{T_{s_i}}}\right) \\ \tanh\left(\frac{\hat{\delta}_{T_{s_i}}^z - \beta_{s_i}(z_{s_i})}{\delta_{T_{s_i}}}\right) \end{bmatrix} \quad (13)$$

where we have considered

$$\begin{aligned} e_{s_i}^1 &= \begin{bmatrix} e_{s_i}^{1x} & e_{s_i}^{1y} & e_{s_i}^{1z} \end{bmatrix}^\top \\ e_{s_i}^2 &= \begin{bmatrix} e_{s_i}^{2x} & e_{s_i}^{2y} & e_{s_i}^{2z} \end{bmatrix}^\top \\ \hat{\delta}_{T_{s_i}} &= \begin{bmatrix} \hat{\delta}_{T_{s_i}}^x & \hat{\delta}_{T_{s_i}}^y & \hat{\delta}_{T_{s_i}}^z \end{bmatrix}^\top \end{aligned}$$

Hence, the closed-loop dynamics (6)-(13) takes de following form

$$\begin{aligned} \dot{e}_{s_i}^1 &= e_{s_i}^2 \\ \dot{e}_{s_i}^2 &= \begin{bmatrix} \frac{\epsilon_{s_i}^x}{2} \tanh\left(\frac{2\lambda_{s_i}^{x1}}{\epsilon_{s_i}^{x1}} e^{1x}\right) + \frac{\epsilon_{s_i}^x}{4} \tanh\left(\frac{4\lambda_{s_i}^{x2}}{\epsilon_{s_i}^{x2}} e^{2x}\right) \\ \frac{\epsilon_{s_i}^y}{2} \tanh\left(\frac{2\lambda_{s_i}^{y1}}{\epsilon_{s_i}^{y1}} e^{1y}\right) + \frac{\epsilon_{s_i}^y}{4} \tanh\left(\frac{4\lambda_{s_i}^{y2}}{\epsilon_{s_i}^{y2}} e^{2y}\right) \\ \frac{\epsilon_{s_i}^z}{2} \tanh\left(\frac{2\lambda_{s_i}^{z1}}{\epsilon_{s_i}^{z1}} e^{1z}\right) + \frac{\epsilon_{s_i}^z}{4} \tanh\left(\frac{4\lambda_{s_i}^{z2}}{\epsilon_{s_i}^{z2}} e^{2z}\right) \end{bmatrix} \\ &\quad - \begin{bmatrix} \frac{\epsilon_{s_{i-1}}^x}{2} \tanh\left(\frac{2\lambda_{s_{i-1}}^{x1}}{\epsilon_{s_{i-1}}^{x1}} e^{1x}\right) \\ \frac{\epsilon_{s_{i-1}}^y}{2} \tanh\left(\frac{2\lambda_{s_{i-1}}^{y1}}{\epsilon_{s_{i-1}}^{y1}} e^{1y}\right) \\ \frac{\epsilon_{s_{i-1}}^z}{2} \tanh\left(\frac{2\lambda_{s_{i-1}}^{z1}}{\epsilon_{s_{i-1}}^{z1}} e^{1z}\right) \\ \frac{\epsilon_{s_{i-1}}^x}{4} \tanh\left(\frac{4\lambda_{s_{i-1}}^{x2}}{\epsilon_{s_{i-1}}^{x2}} e^{2x}\right) \\ \frac{\epsilon_{s_{i-1}}^y}{4} \tanh\left(\frac{4\lambda_{s_{i-1}}^{y2}}{\epsilon_{s_{i-1}}^{y2}} e^{2y}\right) \\ \frac{\epsilon_{s_{i-1}}^z}{4} \tanh\left(\frac{4\lambda_{s_{i-1}}^{z2}}{\epsilon_{s_{i-1}}^{z2}} e^{2z}\right) \end{bmatrix} \\ &\quad - (g - \gamma_{s_i}^z) P_i V_i + (g - \gamma_{s_{i-1}}^z) P_{i-1} V_{i-1} \\ &\quad + \eta_{s_i} - \eta_{s_{i-1}} \end{aligned} \quad (14)$$

where

$$\begin{aligned} P_i &= \begin{bmatrix} c\psi_{s_i} & s\psi_{s_i} & 0 \\ c\psi_{s_i} & -c\psi_{s_i} & 0 \\ 0 & 0 & 0 \end{bmatrix}, \\ P_{i-1} &= \begin{bmatrix} c\psi_{s_{i-1}} & s\psi_{s_{i-1}} & 0 \\ c\psi_{s_{i-1}} & -c\psi_{s_{i-1}} & 0 \\ 0 & 0 & 0 \end{bmatrix} \\ V_i &= \begin{bmatrix} t\theta_{s_i} - t\theta_{s_i}^d \\ \frac{t\phi_{s_i} - t\phi_{s_i}^d}{c\phi_{s_i}} \\ 0 \end{bmatrix}, \quad V_{i-1} = \begin{bmatrix} t\theta_{s_{i-1}} - t\theta_{s_{i-1}}^d \\ \frac{t\phi_{s_{i-1}} - t\phi_{s_{i-1}}^d}{c\phi_{s_{i-1}}} \\ 0 \end{bmatrix} \end{aligned}$$

We are in position to state one of the results of this paper.

Proposition 1: Consider a multiagent system composed of two quadrotors, one of them performing as the leader. Assume that A1-A4 hold. Assume that each quadrotor has a local attitude controller that drives the quadrotor's attitude to its desired reference faster than the bandwidth of the desired translational movements. Then, there exists gains ϵ_l^j , λ_l^{j1} , λ_l^{j2} , $\epsilon_{s_1}^j$, $\lambda_{s_1}^{j1}$, $\lambda_{s_1}^{j2}$ $j = x, y, z$ and positive definite matrices Γ_l , Γ_{s_1} such that the leader-follower coordination problem is locally solved.

Proof: From (14) it can be verified that, under the assumption of fast local attitude controllers, the leader-follower closed-loop dynamics is described by the following equations

$$\begin{aligned} \dot{e}_l^1 &= e_l^2 \\ \dot{e}_l^2 &= \begin{bmatrix} \frac{\epsilon_l^x}{2} \tanh\left(\frac{2\lambda_l^{x1}}{\epsilon_l^{x1}} e^{1x}\right) + \frac{\epsilon_l^x}{4} \tanh\left(\frac{4\lambda_l^{x2}}{\epsilon_l^{x2}} e^{2x}\right) \\ \frac{\epsilon_l^y}{2} \tanh\left(\frac{2\lambda_l^{y1}}{\epsilon_l^{y1}} e^{1y}\right) + \frac{\epsilon_l^y}{4} \tanh\left(\frac{4\lambda_l^{y2}}{\epsilon_l^{y2}} e^{2y}\right) \\ \frac{\epsilon_l^z}{2} \tanh\left(\frac{2\lambda_l^{z1}}{\epsilon_l^{z1}} e^{1z}\right) + \frac{\epsilon_l^z}{4} \tanh\left(\frac{4\lambda_l^{z2}}{\epsilon_l^{z2}} e^{2z}\right) \end{bmatrix} \\ &\quad + \eta_l \\ \dot{e}_{s_i}^1 &= e_{s_i}^2 \\ \dot{e}_{s_i}^2 &= \begin{bmatrix} \frac{\epsilon_{s_i}^x}{2} \tanh\left(\frac{2\lambda_{s_i}^{x1}}{\epsilon_{s_i}^{x1}} e^{1x}\right) + \frac{\epsilon_{s_i}^x}{4} \tanh\left(\frac{4\lambda_{s_i}^{x2}}{\epsilon_{s_i}^{x2}} e^{2x}\right) \\ \frac{\epsilon_{s_i}^y}{2} \tanh\left(\frac{2\lambda_{s_i}^{y1}}{\epsilon_{s_i}^{y1}} e^{1y}\right) + \frac{\epsilon_{s_i}^y}{4} \tanh\left(\frac{4\lambda_{s_i}^{y2}}{\epsilon_{s_i}^{y2}} e^{2y}\right) \\ \frac{\epsilon_{s_i}^z}{2} \tanh\left(\frac{2\lambda_{s_i}^{z1}}{\epsilon_{s_i}^{z1}} e^{1z}\right) + \frac{\epsilon_{s_i}^z}{4} \tanh\left(\frac{4\lambda_{s_i}^{z2}}{\epsilon_{s_i}^{z2}} e^{2z}\right) \end{bmatrix} \\ &\quad - \begin{bmatrix} \frac{\epsilon_l^x}{2} \tanh\left(\frac{2\lambda_l^{x1}}{\epsilon_l^{x1}} e^{1x}\right) \\ \frac{\epsilon_l^y}{2} \tanh\left(\frac{2\lambda_l^{y1}}{\epsilon_l^{y1}} e^{1y}\right) \\ \frac{\epsilon_l^z}{2} \tanh\left(\frac{2\lambda_l^{z1}}{\epsilon_l^{z1}} e^{1z}\right) \end{bmatrix} \\ &\quad - \begin{bmatrix} \frac{\epsilon_l^x}{4} \tanh\left(\frac{4\lambda_l^{x2}}{\epsilon_l^{x2}} e^{2x}\right) \\ \frac{\epsilon_l^y}{4} \tanh\left(\frac{4\lambda_l^{y2}}{\epsilon_l^{y2}} e^{2y}\right) \\ \frac{\epsilon_l^z}{4} \tanh\left(\frac{4\lambda_l^{z2}}{\epsilon_l^{z2}} e^{2z}\right) \end{bmatrix} \\ &\quad + \eta_{s_1} - \eta_l \end{aligned} \quad (15)$$

together with the disturbance estimation error dynamics

$$\begin{aligned} \dot{\eta}_l &= -\Theta_l \Gamma_l \eta_l \\ \dot{\eta}_{s_1} &= -\Theta_{s_1} \Gamma_{s_1} \eta_{s_1} \end{aligned} \quad (16)$$

Note that the dynamics described by equations (15) and (16)

can be written as a cascade system of the form

$$\begin{aligned}\dot{z}_e &= g(z_e) \\ \dot{x}_e &= f(x_e) + h(z_e)\end{aligned}$$

with

$$\begin{aligned}z_e &= [\eta_l \quad \eta_{s1}]^\top \\ x_e &= [e_l^1 \quad e_l^2 \quad e_{s1}^1 \quad e_{s1}^2]^\top \\ h(z_e) &= [0_{3 \times 1} \quad \eta_l \quad 0_{3 \times 1} \quad \eta_{s1} - \eta_l]^\top\end{aligned}$$

Note that the interconnection term $h(z_e)$ satisfies the linear growth condition [22] for cascade systems. Moreover, it can be verified that, at least, locally $g(z_e)$ and $f(x_e)$ satisfy the necessary and sufficient conditions to guarantee local stability of the cascade system. This proves that the leader-follower coordination problem is locally solved. ■

IV. REAL-TIME IMPLEMENTATION

A. Hardware setup

The hardware setup consists of the positioning system from Optitrack, based on infrared cameras, and two quadrotors, see Figure 3. Each quadrotor has a control system based on a Digital Signal Processor from Texas Instruments, an inertial measurement unit (IMU) from Xsens and two WiFly modules from Roving Networks. The positioning system sends to each quadrotor the position of its center of gravity as well as the emergency stop digital signal by means of the TCP/IP protocol. The quadrotor leader sends the position of its center of gravity as well as a synchronization signal to the follower also by means of the TCP/IP protocol using a point to point network. The Digital Signal Processors compute the local nonlinear quadrotor controllers onboard.

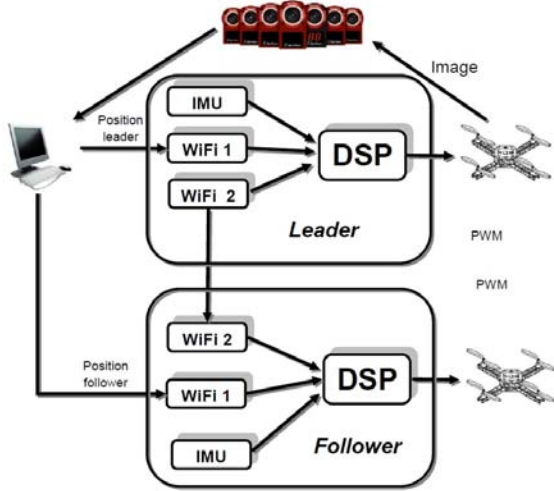


Fig. 3. Leader-Follower implementation

B. Real time algorithm

The real time algorithm is based on the Giotto methodology for embedded systems [13]. This methodology has been already used to implement nonlinear quadrotor controller in

[10]. Here, we just plug the new tasks which are necessary for the leader to broadcast its position and the synchronization signal and for the follower to receive both signals.

For the leader-follower scheme two modes are defined. The *mode 1* or *star mode*, this mode performs the initialization of all the sensors (positioning system, IMU) and the communication between the leader and the follower. The *mode 2* also called *Autonomous flight mode* performs the operation of the quadrotor in autonomous flight. In this mode, the local control laws are computed and the communication link between the leader and the follower is active. Both modes are shown in Figure 4 and the description of the tasks is presented in Table 1.

| Task | Input | Output |
|----------|--------------------------------|------------------------------|
| t_1 | i_1 Φ string format | o_1 Φ string format |
| t_2 | i_2 Ω string format | o_2 Ω string format |
| t_3 | i_4 X string format | o_3 X string format |
| t_4 | i_5 X string format | o_4 X string format |
| t_5 | i_8 X float format | o_6 Φ_d float format |
| t_6 | i_{10} Φ_d float format | o_7 PWM integer format |
| t_7 | i_7 PWM analog signal | o_5 integer format |
| t_8 | i_{13} X_L string format | o_9 X string format |
| t_9 | i_{14} bit | o_{10} bit |
| t_{10} | i_{15} bit | o_{11} bit |
| t_{11} | i_{16} bit | o_{12} bit |
| t_{12} | i_{17} bit | o_{13} bit |

Table 1. Input/output of each task.

In Table 1, t_1 reads Euler Angles data from IMU, t_2 reads angular velocities from IMU, t_3 reads Cartesian position block one, t_4 reads Cartesian position block two, t_5 computes the position control, t_6 computes the attitude control, t_7 monitors the emergency stop signal, t_8 receives the leader position, t_9 synchronizes the IMU, t_{10} synchronizes the WiFi communication, t_{11} synchronizes the leader and t_{12} synchronizes the clock.

Finally, the position is obtained at 60 Hz, the attitude and rotational velocity are obtained at 120Hz, the leader broadcast its position at 60Hz and the aerodynamic actuators are refreshed at 400Hz.

V. EXPERIMENTAL RESULTS

In order to test the performance of the proposed coordination scheme we carried out two experiments. In the first one the leader follows a continuous trajectory parameterized in time with continuous first and second time derivatives. For the second experiment the leader goes to three way points without planning the references for velocity and acceleration.

The numerical values of the quadrotor helicopter parameters are summarized in Table 2.¹

¹When it is not explicitly stated, we considered the same value for the leader and the follower.

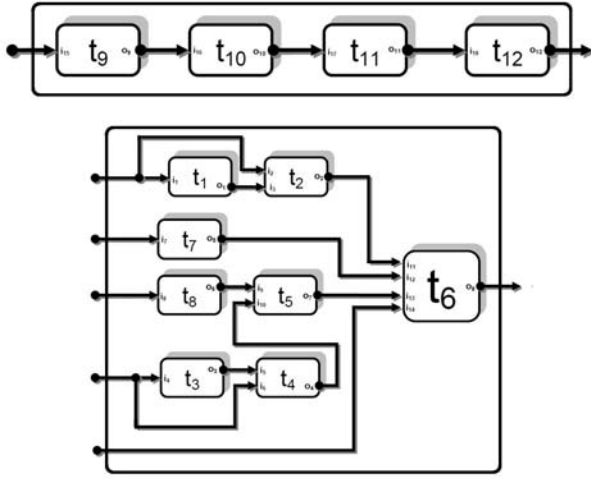


Fig. 4. Giotto Model

| Parameter | Value | Parameter | Value |
|-------------------------------|------------|-------------------------------|-------|
| m_l, m_{s_1} (kg) | 0.9, 1.120 | ℓ (m) | 0.214 |
| g (m/s ²) | 9.81 | I_{xx} (kg m ²) | 0.002 |
| I_{yy} (kg m ²) | 0.002 | I_{zz} (kg m ²) | 0.004 |

Table 2. Quadrotor helicopter parameters

For the first experiment the desired trajectory was defined as the Bernoulli lemniscate, which parameterized with respect to time is described by the following equations.

$$\begin{aligned} x_d &= \frac{1.5 \sin(t\omega_t) \cos(t\omega_t)}{1 + \cos(t\omega_t)^2} \\ y_d &= \frac{1.5 \sin(t\omega_t)}{1 + \cos(t\omega_t)^2} \\ z_d &= -3 - 0.7 \sin(t\omega_t) \end{aligned} \quad (17)$$

and the interagent distance vector defined by

$$\alpha_{s,l} = [2.4 \quad 1 \quad 0]^\top$$

The parameters of the local controllers for the leader and the follower are presented in Table 3.

| Parameter | Value | Parameter | Value |
|--|----------|--|-----------|
| $\gamma_l^x, \gamma_{s_1}^x$ | 1.4, 1.2 | $\delta_l^x, \delta_{s_1}^x$ | 1.5, 1.5 |
| $\gamma_l^y, \gamma_{s_1}^y$ | 1.2, 1.4 | $\delta_l^y, \delta_{s_1}^y$ | 3.0, 3.0 |
| $\gamma_l^z, \gamma_{s_1}^z$ | 2.0, 2.0 | $\delta_l^z, \delta_{s_1}^z$ | 2.0, 2.0 |
| $\epsilon_l^x, \epsilon_{s_1}^x$ | 80, 80 | $\delta_l^x, \delta_{s_1}^x$ | 0.4, 0.05 |
| $\epsilon_l^y, \epsilon_{s_1}^y$ | 80, 80 | $\delta_l^y, \delta_{s_1}^y$ | 0.4, 0.05 |
| $\epsilon_l^z, \epsilon_{s_1}^z$ | 11, 11 | $\delta_l^z, \delta_{s_1}^z$ | 0.2, 0.02 |
| $\lambda_l^{x_1}, \lambda_{s_1}^{x_1}$ | 2.0, 2.0 | $\lambda_l^{y_1}, \lambda_{s_1}^{y_1}$ | 2.0, 2.0 |
| $\lambda_l^{x_2}, \lambda_{s_1}^{x_2}$ | 4.0, 4.0 | $\lambda_l^{y_2}, \lambda_{s_1}^{y_2}$ | 4.0, 4.0 |

Table 3. Controller parameters

Figure 5 presents the trajectory followed by the leader while Figure 6 presents the trajectory traveled by the follower. As it can be observed the follower performs not as well as the leader, this is because the position of the leader is not as smooth as the signal computed from the desired trajectory.

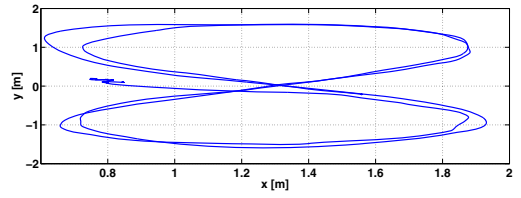


Fig. 5. Leader

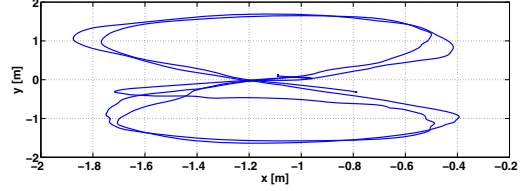


Fig. 6. Follower

For the second experiment the waypoints were defined as

$$\begin{aligned} W_1 &= [1.5 \quad 1.4 \quad -0.4]^\top \\ W_2 &= [0 \quad 1 \quad -0.4]^\top \\ W_3 &= [1 \quad -0.5 \quad -0.4]^\top \end{aligned}$$

Figure 7 shows the performance of the leader-follower coordination scheme traveling through waypoints. Finally, Figure

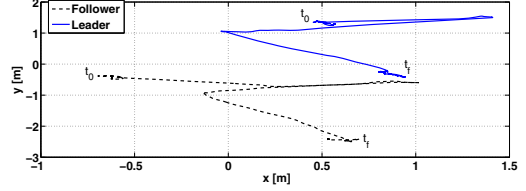


Fig. 7. Leader follower coordination traveling through waypoints.

8 shows a picture of the two quadrotors in flight.

VI. CONCLUSION

We have presented a decentralized real time implementation of a leader follower coordination scheme using quadrotors. The local stability properties of the resulting closed-loop dynamics have been established. The performance of the coordination scheme is verified experimentally.

REFERENCES

- [1] Saifa Al-Hiddabi. Quadrotor control using feedback linearization with dynamic extension. In *Mechatronics and its Applications, 2009. ISMA'09. 6th International Symposium on*, pages 1–3. IEEE, 2009.
- [2] A. Astolfi, D. Karagiannis, and R. Ortega. *Nonlinear and Adaptive Control with Applications*. Communications and Control Engineering. Springer, 2007.
- [3] Ismail Bayezit and Baris Fidan. Distributed cohesive motion control of flight vehicle formations. *Industrial Electronics, IEEE Transactions on*, 60(12):5763–5772, 2013.
- [4] Pedro Castillo, Rogelio Lozano, and Alejandro Dzul. Stabilization of a mini rotorcraft with four rotors. *IEEE Control Systems Magazine*, 25(6):45–55, 2005.



Fig. 8. Leader follower coordination.

- [5] Abbas Chamseddine, Youmin Zhang, Camille Alain Rabbath, Cedric Join, and Didier Theilliol. Flatness-based trajectory planning/replanning for a quadrotor unmanned aerial vehicle. *Aerospace and Electronic Systems, IEEE Transactions on*, 48(4):2832–2848, 2012.
- [6] R. Castro D. A. Mercado and R. Lozano. Quadrotors flight formation control using a leader-follower approach. In *2013 European Control Conference (ECC)*, pages 3858–3863, 2013.
- [7] Khac Duc Do. Formation tracking control of unicycle-type mobile robots with limited sensing ranges. *Control Systems Technology, IEEE Transactions on*, 16(3):527–538, 2008.
- [8] Sergio Araujo Estrada, Eduardo Liceaga-Castro, and H Rodriguez-Cortes. Nonlinear motion control of a rotary wing vehicle powered by four rotors. In *Electrical and Electronics Engineering, 2006 3rd International Conference on*, pages 1–6. IEEE, 2006.
- [9] J Alexander Fax and Richard M Murray. Information flow and cooperative control of vehicle formations. *Automatic Control, IEEE Transactions on*, 49(9):1465–1476, 2004.
- [10] J Rogelio Guadarrama-Olvera, José J Corona-Sánchez, and H Rodríguez-Cortés. Hard real-time implementation of a nonlinear controller for the quadrotor helicopter. *Journal of Intelligent & Robotic Systems*, 73(1-4):81–97, 2014.
- [11] Nicolas Guenard, Tarek Hamel, and Robert Mahony. A practical visual servo control for an unmanned aerial vehicle. *Robotics, IEEE Transactions on*, 24(2):331–340, 2008.
- [12] Tarek Hamel, Robert Mahony, Rogelio Lozano, and James Ostrowski. Dynamic modelling and configuration stabilization for an x4-flyer. *aa*, 1(2):3, 2002.
- [13] Thomas A Henzinger, Benjamin Horowitz, and Christoph Meyer Kirsch. Giotto: A time-triggered language for embedded programming. In *Embedded Software*, pages 166–184. Springer, 2001.
- [14] Rafael Castro-Linares J. Rogelio Guadarrama-Olvera, Hugo Rodríguez-Cortés. Robust trajectory tracking control of a quadrotor helicopter. In *submitted to 2014 European Control Conference*, pages 84–89, 2014.
- [15] H. Rodríguez-Cortés José J. Corona-Sanchez. Path following control for the cartesian position of the quadrotor. In *Conferencia Latinoamericana de Control Automático, Lima, Peru*, 2012.
- [16] DongBin Lee, Timothy C Burg, Bin Xian, and Darren M Dawson. Output feedback tracking control of an underactuated quad-rotor uav. In *American Control Conference, 2007. ACC'07*, pages 1775–1780. IEEE, 2007.
- [17] M Anthony Lewis and Kar-Han Tan. High precision formation control of mobile robots using virtual structures. *Autonomous Robots*, 4(4):387–403, 1997.
- [18] Peng Lin, Kaiyu Qin, Zhongkui Li, and Wei Ren. Collective rotating motions of second-order multi-agent systems in three-dimensional space. *Systems & Control Letters*, 60(6):365–372, 2011.
- [19] Guilherme V Raffo, Manuel G Ortega, and Francisco R Rubio. An integral predictive/nonlinear \mathcal{H}_∞ structure for a quadrotor helicopter. *Automatica*, 46(1):29–39, 2010.
- [20] Wei Ren and Randal W Beard. Consensus algorithms for double-integrator dynamics. *Distributed Consensus in Multi-vehicle Cooperative Control: Theory and Applications*, pages 77–104, 2008.
- [21] S Salazar-Cruz, A Palomino, and R Lozano. Trajectory tracking for a four rotor mini-aircraft. In *Decision and Control, 2005 and 2005 European Control Conference. CDC-ECC'05. 44th IEEE Conference on*, pages 2505–2510. IEEE, 2005.
- [22] R Sepulchre, M Jankovic, and PV Kokotovic. *Constructive nonlinear control, 1997*. Springer, Berlin, 1997.
- [23] Matthew Turpin, Nathan Michael, and Vijay Kumar. Trajectory design and control for aggressive formation flight with quadrotors. *Autonomous Robots*, 33(1-2):143–156, 2012.
- [24] Steven Lake Waslander, Gabriel M Hoffmann, Jung Soon Jang, and Claire J Tomlin. Multi-agent quadrotor testbed control design: Integral sliding mode vs. reinforcement learning. In *Intelligent Robots and Systems, 2005.(IROS 2005). 2005 IEEE/RSJ International Conference on*, pages 3712–3717. IEEE, 2005.
- [25] Wenwu Yu, Wei Xing Zheng, Guanrong Chen, Wei Ren, and Jinde Cao. Second-order consensus in multi-agent dynamical systems with sampled position data. *Automatica*, 47(7):1496–1503, 2011.